ACTA ABP BIOCHIMICA POLONICA

Vol. 62, No 2/2015
221–227
http://dx.doi.org/10.18388/abp.2014_920

Regular paper

Characterization of ATPase activity of the AAA ARC from *Bifidobacterium longum* subsp. *infantis*

Mabel Guzmán-Rodríguez, Ana Paulina Barba de la Rosa and Leticia Santos✉

División de Biología Molecular, Instituto Potosino de Investigación Científica y Tecnológica, A.C. (IPICYT), CP 78216 San Luis Potosí, México

Bifidobacteria are considered to be probiotics that exist in the large intestine and are helpful to maintain human health. Oral administration of bifidobacteria may be effective in improving the intestinal flora and environment, stimulating the immune response and possibly preventing cancer. However, for consistent and positive results, further well-controlled studies are urgently needed to describe the basic mechanisms of this microorganism. Analysis of the proteasome-lacking *Bifidobacterium longum* genome reveals that it possesses a gene, *IPR003593 AAA ATPase core*, which codes a 56 kDa protein containing one AAA ATPase domain. Phylogenetic classification made by CLANS, positioned this sequence into the ARC divergent branch of the AAA ATPase family of proteins. N-terminal analysis of the sequence indicates this protein is closely related to other ATPases such as the *Rhodococcus erythropolis* ARC, *Archaeoglobus fulgidus* PAN, *Mycobacterium tuberculosis* Mpa and the human proteasomal Rpt1 subunit. This gene was cloned, the full-length recombinant protein was overexpressed in *Escherichia coli*, purified as a high-molecular size complex and named Bl-ARC. Enzymatic characterization showed that Bl-ARC ATPase is active, Mg^{+2}-dependent and sensitive to *N*-ethylmaleimide. Gene organization positions *bl-arc* in a region flanked by a cluster of genes that includes *pup*, *dop* and *pafA* genes. These findings point to a possible function as a chaperone in the degradation pathway *via* pupylation.

Key words: *Bifidobacterium longum*; ARC; AAA ATPase; probiotic

Received: 15 October, 2014; revised: 08 May, 2015; accepted: 11 May, 2015; available on-line: 26 May, 2015

INTRODUCTION

Lactic acid bacterium *Bifidobacterium longum* was isolated and described over a century ago from human infant feces and was associated with a healthy intestinal tract in humans (Tissier, 1900). This flora protects the intestinal tract from proliferation or infection by harmful bacteria; recent research has focused on bifidobacteria to establish the importance of these organisms in influencing certain normal functions of the intestinal tract and in exploring their role in the human health.

Evidence of the previous observations was described in a report where dietary administration of lyophilized cultures of *B. longum* suppressed colon and mammary carcinogenesis in laboratory animal models (Reddy, 1999), while another describes that bifidobacteria have effects on the treatment of rotavirus diarrhea (Marteau *et al.*, 1990). Daily oral administration of bifidobacteria, oligofructose and inulin also produced an anti-inflammatory effect in a rat model of acute colitis induced by DSS (Osman *et al.*, 2006). Lastly, ingestion of bifidobacteria culture may stimulate the immune response (Hiramatsu *et al.*, 2011).

The relationship of *B. longum* with its host provides a myriad of unexplored biological mechanisms. Since experimental evidence of the effectiveness of bifidobacteria is limited, it is urgent to study the basic molecular mechanisms underlying the health-promoting features, especially in complex phenomena as anti-carcinogenic or anti-inflammatory effects. Due to the importance of the aforementioned characteristics, the probiotic *B. longum* is subject to global analyses such as genome sequencing, genome variations (Bar-Nun & Glickman, 2012; Hao *et al.*, 2011), Delcenserie *et al.*, 2008; Guy *et al.*, 2005; Schell *et al.*, 2002; Sela *et al.*, 2008) (Shkoporov *et al.*, 2013; Yu *et al.*, 2013; Zhurina *et al.*, 2013) and proteomics (Olivares *et al.*, 2011; Ruiz *et al.*, 2009; Sun *et al.*, 2008; Yuan *et al.*, 2006; Zhao & Cheung, 2013).

Molecular chaperones are key in maintaining protein quality, especially under stress conditions; however, the role of these proteins in *B. longum* has not been studied yet. In eukaryotes, the mechanisms of protein control (PC) are provided by machineries (Doyle *et al.*, 2013) (DeMartino, 2009) exemplified by the ubiquitin-proteasome system (UPS) (Tanaka, 2009) or the PAN-proteasome system described in archaea (Benaroudj *et al.*, 2003). In Gram-negative bacteria (e.g. *Escherichia coli*), chaperones such as ClpA or ClpX and the proteases ClpP (forming the ClpAP and ClpXP complexes), ClpYQ, FtsH and Lon are the molecules related to the PC (Kress *et al.*, 2009). Particularly, Gram-positive actinobacteria such as *Rhodococcus*, *Streptomyces*, *Frankia* and *Mycobacterium* genus (Barandun *et al.*, 2012) contain proteasomal subunits which are coupled with a set of chaperones such as Pup, ARC/Mpa, Dop and PafA, forming a mechanism called pupylation (Striebel *et al.*, 2009a; Striebel *et al.*, 2009b) (Cerda-Maira *et al.*, 2010) (Samanovic *et al.*, 2013). Specifically, the AAA ATPase ARC was first described in *Rhodococcus erythropolis* (ReARC) (Wolf *et al.*, 1998) and later in *Mycobacterium tuberculosis* (Mpa) (Wang *et al.*, 2009)2009. ARC (Mpa) proteins are homohexameric ring protein complexes with chaperone activity.

B. longum belongs to a distinctive subclass of actinobacteria (bifidobacteria) that are proteasome-lacking or-

✉e-mail: lsantos@ipicyt.edu.mx

Abbreviations: AAA, ATPases Associated to a variety of distinct Activities; ARC, AAA ATPase forming ring-shaped complexes.

ganisms (Zhang *et al.*, 2004). In general, bifidobacteriales conserve the set of chaperones such as the trigger factor, small Hsp, GroEL/GroES, DnaK/DnaJ/GrpE, and ClpB (Sugimoto & Sonomoto, 2011) that substitute the UPS. We found that *B. longum* genome has the *arc* and accessory genes for the mechanism of pupylation (*pup*, *pafA* and *dop* genes).

In this work we describe the cloning, expression and biochemical characterization of the AAA ATPase ARC from *B. longum* with the intention to know if the coding sequence of the *arc* gene is active for subsequent functional studies.

MATERIALS AND METHODS

Sequence analysis and 3D structure. Homologues of the *B. longum arc* sequenced open reading frames were identified using the BLAST tool server at the NCBI (www.blast.ncbi.nlm.nih.gov/). Sequence alignments were done using the Clustal W application program. CLustal ANalysis of Sequences (CLANS) Program was used to detect families of related proteins in a large set of AAA sequences (Frickey & Lupas, 2004). 3D structure prediction was performed by using the I-TASSER server (Roy *et al.*, 2010; 2012; Zhang, 2008) and the UCSF-Chimera

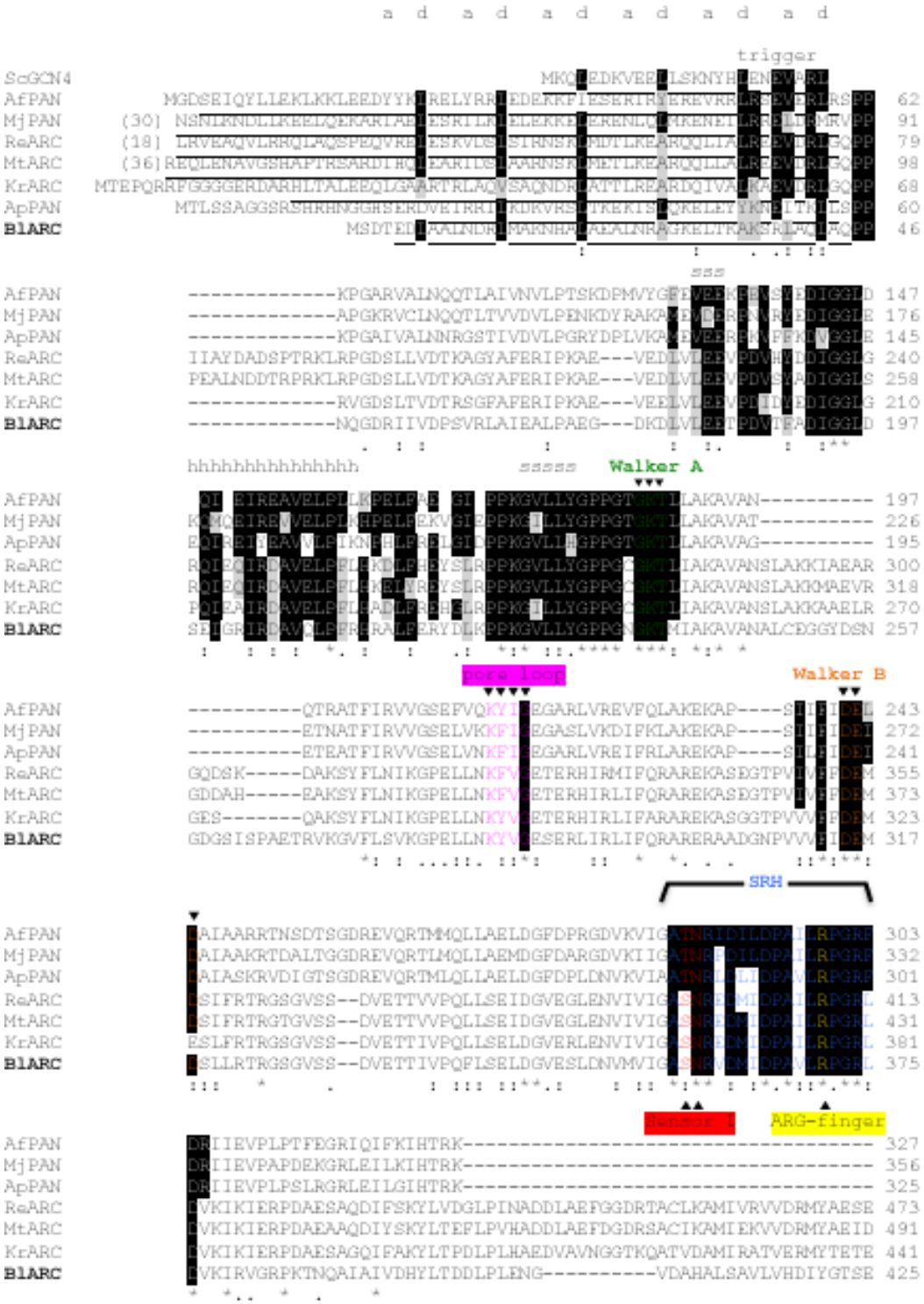

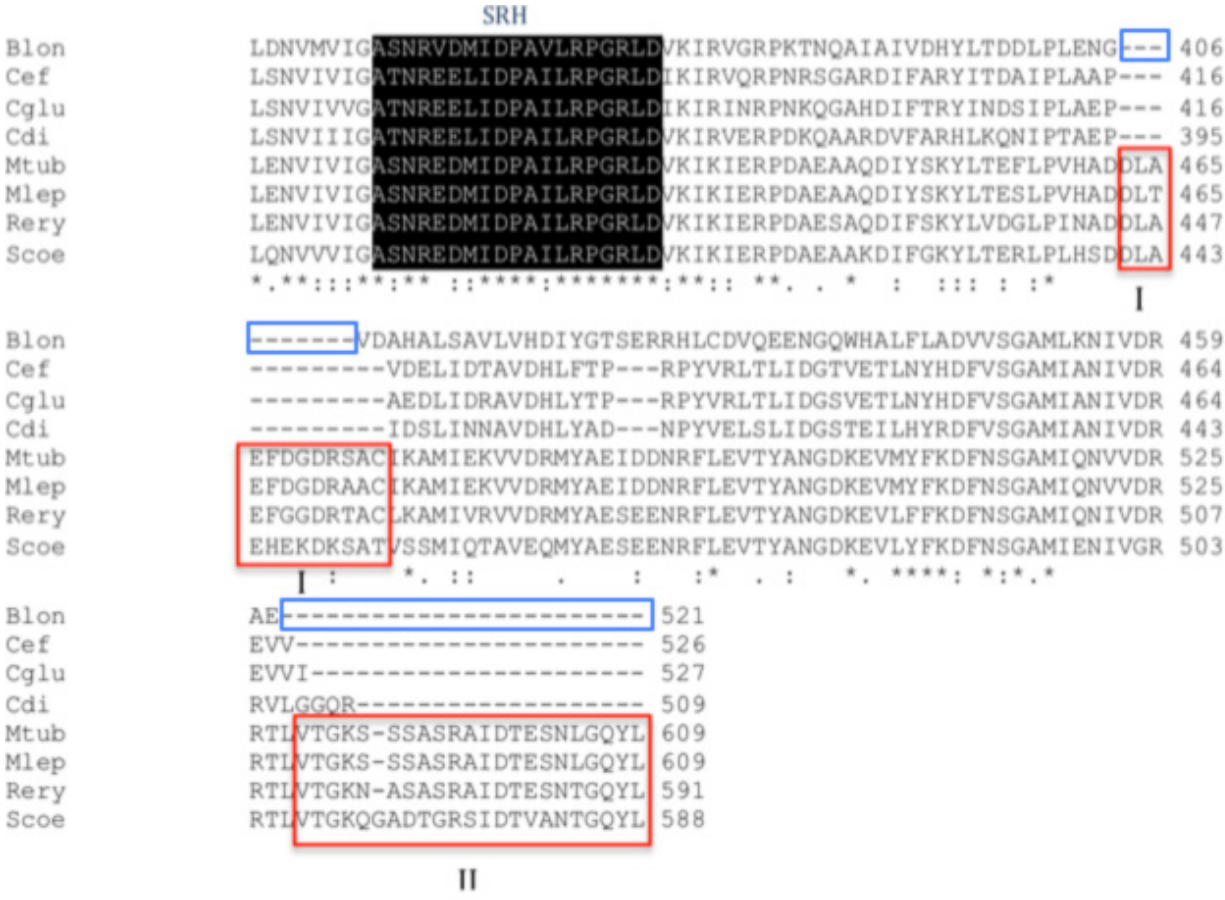

Figure 1. Alignment of *B. longum* ARC with representative members of proteasomal ATPases.
(**Top**) For the coiled-coil structures, the positions of the hydrophobic core residues are marked (**a, d**), and the regions predicted to assume coiled-coil structure in the individual sequences are underlined; the sequence of the ScGCN4 leucine zipper is included for reference, and the location of the trigger sequence essential for folding is indicated. (**Middle**) The consensus secondary structure is shown as s = beta strand and h = alpha helix. (**Bottom**) The AAA domain is shown Walker A/B and Sensor 1 motif, the arginine residue predicted to act as an arginine finger, as well as the pore loop, are indicated in the alignment with arrows; Second Region of Homology (SRH) is shown in the upper text with a black line. Residues conserved in the aligned sequences are highlighted in black and similar residues are highlighted in grey. A box at the C-terminal end of the Bl-ARC sequence is depicted indicating the lacking-proteasome interacting region. AfPAN (*Archaeoglobus fulgidus* gi 3122632), MjPAN (*Methanocaldococcus jannaschii* gi 2492524), ReARC (*Rhodococcus erythropolis* gi 3790601), MtARC (*Mycobacterium tuberculosis* gi 15841607), KrARC (*Kineococcus radiotolerans* gi 69285208), ApPAN (*Aeropyrum pernix* gi 20532220) and BlARC (*Bifidobacterium longum* subsp. *infantis* gi 213524442. (**b**) ARC proteins from proteasome-lacking organisms: Blon, *Bifidobacterium longum* subsp. *infantis*; Cef, *Corynebacterium efficiens*; Cdi, *C. diphtheriae*; Cglu, *C. glutamicum*. Microorganisms containing proteasome genes contain regions in ARC that interact with the proteasome α-subunit (boxes I and II): Mlep, *M. leprae*; Mtub, *M. tuberculosis*; Rery, *R. erythropolis*; Scoe, *S. coelicolor*.

program for interactive analyses of the structures (Meng *et al.*, 2006).

Bacterial strain and cell culture. The *B. longum subsp. infantis* strain (DSMZ 20088) was purchased from the Leibniz-Institute DSMZ-German Collection of Microorganisms and Cell Cultures. *B. longum* was grown in a CO_2 chamber at 37°C in MRS medium containing 1 g peptone, 1 g beef extract, 0.5 g yeast extract, 0.1 g Tween 80, 0.2 g ammonium citrate, 0.5 g sodium acetate, 0.01 g $MgSO_4$, 0.005 g $MnSO_4$, 0.2 g K_2HPO_4, 2 g glucose and 0.05 g cysteine in 100 mL distillated water for three days.

DNA isolation. *B. longum* culture was harvested by centrifugation at 6000 × *g* for 15 min at room temperature. Cell pellet was resuspended in the presence of 10 μg/μL lysozyme, 20 mg/ml proteinase K and 2 mg/ml zymolyase, for 30 min on ice. After incubation, phenol/chloroform/isoamyl alcohol was added and stirred for 10 min. To separate the two phases (aqueous/organic) the samples were harvested at 5400 g for 10 min. The aqueous layer was transferred to a fresh tube and 70% ethanol was added. Centrifugation was then performed at 5400 g for 6 min to pellet the DNA. This washing step was repeated once. The pellet was air-dried for 5 min and resuspended in 30 μL sterile Milli-Q-water.

Cloning, heterologous expression in *E. coli* and immunoblotting. Amplification of the *bl-arc* gene (IPR003593 AAA+ ATPase core ORF) was performed with a pair of the following oligonucleotides: 5'-ATGAGCGACACCGAAGATCTCG-3' and 5'-TTCGGCGGTGCGGATGCGGC-3' and *B. longum* genomic DNA. To add a coding C-terminally fused His6-tag to the *bl-arc* gene into the phage T7 promoter-based expression pET28a(+) vector, we used the *Nde*I and *Xho*I sites at the 5' and 3' terminal ends: 5'-GGGGAATTCCATATGAGCGACACCG-3' and 5'-CTCTCGAGTTCGGCGGTGCGGATG-3'. PCR was done in a 50 μL reaction in the presence of *Pfx* polymerase (Invitrogen) using the following conditions: 94°C for 5 min, 30 cycles of 94°C for 30 s, 55°C for 30 s, 68°C for 2 min; and a final extension at 68°C for 10 min. The PCR product

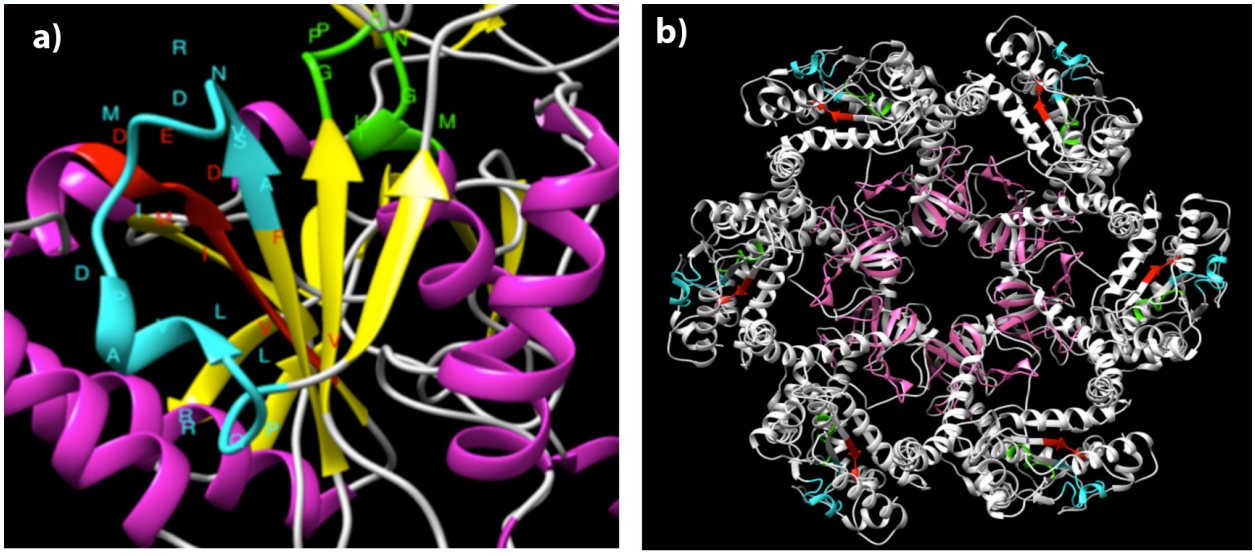

Figure 2. The overall 3D structure prediction of the AAA Bl-ARC obtained by homology modeling.
(**a**) Composition of the ATP binding domains. The Walker motif A and B segments are colored green and cyan respectively, and the SRH is in magenta. (**b**) Complete assembly of the hexameric ring. This prediction was conducted using the *Mtb* ARC crystal interdomain.

was cloned into the pCR4-TOPO TA vector and transformed into the host strain *E. coli XL1 blue* (Invitrogen). This construct was digested with *Nde*I and *Xho*I (Invitrogen) and ligated into a *NdeI*/*XhoI* pET28a(+) vector sites. The pET28a(+)-*bl-arc* construct was used to transform *E. coli* BL21(DE3) pLysS cells. Cell culture was grown in 500 mL of LB medium in the presence of kanamycin (50 mg/mL) and chloramphenicol (35 mg/mL) at 28°C and induced with 1 mM IPTG until the optical density reached 0.6 at a wavelength of 600 nm. The cells were harvested at 13000 rpm at 4°C for 20 minutes. The cell pellet was resuspended in lysis buffer (50 mM $Na_2H_2PO_4$, 300 mM NaCl, pH 8.0), sonicated and pelleted again at 13000 rpm for 20 minutes. The recombinant Bl-ARC protein was purified by affinity chromatography on Ni-NTA spin columns (Qiagen) under native conditions. Protein concentration was determined by using the Bio-Rad Protein Assay Solution and bovine serum albumin was used as a protein standard. To confirm the theoretically calculated molecular mass and the state of oligomerization, proteins were analyzed on a 10% SDS/PAGE and 5–15% native gradient gels. Bands were stained using the colloidal Coomassie method (R250, BioRad). The crude extract and purified protein were blotted from SDS or native gels onto nitrocellulose. Membranes were probed with an anti-His mouse monoclonal antibody conjugated with alkaline phosphatase (AbD Serotec) and antigen-antibody complexes were visualized by using alkaline phosphatase-conjugated anti-mouse IgG antibodies (Invitrogen) developed with NBT and BCIP (Amersham Bioscience).

Mass spectrometry. Bl-ARC was identified by mass spectrometry analysis (LC-ESI-MS/MS) in the LINAN laboratory facility at IPICYT. Data analysis was performed on the MS/MS spectra datasets using the MASCOT search algorithm (Matrix Science, London, UK). Searches were conducted using the NCBI database.

ATPase activity assay. ATPase characterization was assayed by measuring the release of inorganic phosphate from ATP, by the method of Lanzetta and coworkers (Lanzetta *et al.*, 1979). Triplicate reactions containing 10 µg of the recombinant Bl-ARC in a buffer containing 50 mM MES, pH 5.0, 100 mM NaCl, 10 mM of several divalent cation metals, and 1 mM nucleotide were incubated for 15 min at 37°C. Negative control reactions in the absence of the enzyme, also in triplicate, were performed in parallel. Kinetic parameters, K_m and V_{max} were determined within the first ten minutes of the assay by measuring the initial velocity of ATP hydrolysis. These parameters were calculated using the KaleidaGraph program (Synergy Software).

RESULTS AND DISCUSSION

Sequence analysis, phylogenetic classification and 3D structure

Deduced amino acid sequence analysis of the IPR003593 AAA+ ATPase core ORF showed 40% identity to the ARC AAA ATPase from *R. erythropholis* (Genbank AAC6869.1) and *Streptomyces coelicor* (Genbank AAC64282.1). Database searches displayed a wide number of ARC homologs (Zhang *et al.*, 2004). BLAST searches and multiple sequence alignment confirmed high sequence similarity against chaperones involved in the degradation pathway *via* proteasome such as archaeal PAN (Smith *et al.*, 2005) and the human Rpt1 proteasomal subunit (Bar-Nun & Glickman, 2012) (Fig. 1). The analysis revealed presence of a single AAA family domain where the Walker A region covers the residues Gly232 to Leu240, the Walker B from Iso311 to Glu316 and the SRH from Ala358 to Asp376. As depicted in Fig. 1, the sequence contains an N-terminal coiled coil considered important for possible binding and recognition of target proteins in the degradation process (Djuranovic *et al.*, 2009) (Met1 to Pro46). This region contains three conserved leucine residues in positions 7, 14, 21 and one Ala28. Likewise, other conserved amino acids, Ala35, Lys36, Leu39, Leu42, Pro45 and Pro46 are present at the N-terminal substrate recognition domain of proteasomal ATPases (Djuranovic *et al.*, 2009). As expected, sequence analysis of the C-termini clearly shows the two missing regions required for the interaction with proteasome (box I and II). This feature has been reported for *Corynebacterium efficiens, C. diphtheriae,* and *C. glutamicum* (Zhang *et al.*, 2004) (Fig. 1).

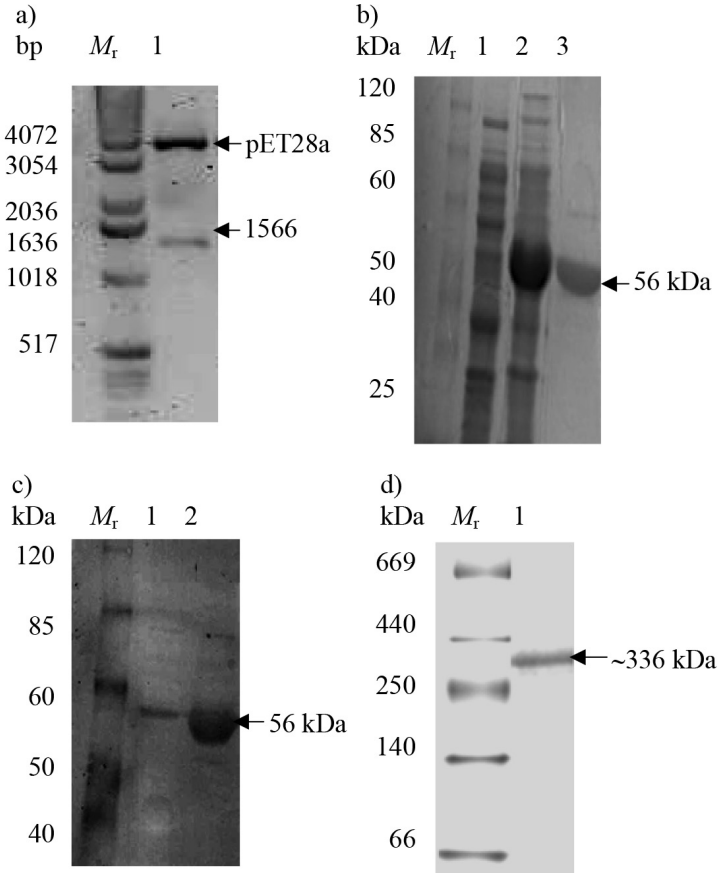

Figure 3. (a) Cloning of the IPR003593 ORF (*bl-arc*).
1% agarose gel analysis. M_r, 1 kb DNA ladder (Invitrogen); Lane 1, Digestion with *Nde*I and *Xho*I restriction enzymes showing the release of the *bl-arc* insert (1566 bp) from the pET28a(+) vector (3956 bp).
(b) Expression analysis of the recombinant Bl-ARC in *E. coli* BL21pLysS in 10% SDS/PAGE gel stained with Coomassie blue.
M_r, Benchmark M_r ladder (Invitrogen); lane 1, Non-induced *E. coli* cells; lane 2, Bl-ARC over-expression with 1 mM IPTG (4 hours); lane 3, Ni-NTA purified recombinant Bl-ARC.
(c) Western blot analysis of the recombinant protein using anti-His tagged antibodies.
M_r, Benchmark M_r ladder (Invitrogen); lane 1, purified recombinant protein, lane 2, soluble fraction after IPTG induction.
(d) Native PAGE.
M_r, Calibration kit for native electrophoresis (Amersham); lane 1, purified recombinant Bl-ARC.

CLANS' analysis (Frickey & Lupas, 2004) was computed against 10 000 AAA proteins covering all subfamilies of the AAA ATPase. The tree confirmed the IPR003593 AAA+ ATPase core deduced amino acid sequence to be a part the ARC subgroup in the phylogenetic dendrogram; thus we termed this molecule as Bl-ARC.

A 3D model of Bl-ARC was constructed based on the homology of AAA published structures from *M. tuberculosis* ARC and *Mus musculus* p97. Homology modeling was predicted against the Protein Data Bank (http://www.rcsb.org) using the I-TASSER server. The server returned a model using the X-ray crystal structure of the AAA protein p97 (PDB ID: 3CF1) as a template. We obtained the best hit: 0.52 TM-score against Bl-ARC that indicates the global structural similarity between both structures (a TM-score > 0.5 indicates a model of correct topology *vs* TM-score < 0.17 means random similarity) (Xu & Zhang, 2010). Moreover, we obtained a C-score of 0.33; this value confirmed the quality of the predicted model (range 0 to 1; higher value indicates more confidence). Lastly, the RMSD score (root-mean-square deviation of atomic positions) of 5.35 denoted a high average distance between the atoms of the superimposed proteins (Roy *et al.*, 2010).

The visualization of the structure was obtained with the USFC-Chimera program. We found that the N-terminal domain in Bl-ARC is composed of five parallel beta strands (β5, β1, β4, β3, β2) flanked by alpha helices as reported for other AAA proteins (Ogura & Wilkinson, 2001; Reuter *et al.*, 2004). In the ARC proteins this region assists the chaperone activity by mediating interactions with Pup proteins in the pupylation mechanism (Sutter *et al.*, 2009).

Crystal structures of hexameric AAA proteins such as HsIU, FtsH, LonB and ClpX have been reported by their importance in protein processing. This conformation plays a crucial role in mechanistic events such as upon ATP hydrolysis that allows substrates to adjust and unfold; the substrates can be then translocated through the pore of the hexameric ring (Vale, 2000).

The hexameric structure of Bl-ARC was therefore modeled, considering the interdomain crystal structure described for *M. tuberculosis* (PDB 3M9B) that is 28% similar to Bl-ARC (Fig. 2). Results of this model suggest a close functional relationship between Bl-ARC and proteins that target substrates for degradation.

Expression of recombinant Bl-ARC and state of oligomerization

Sequencing of the positive clones with the *bl-arc* gene confirmed an inserted DNA of 1566 bp in length corresponding to the expected size by agarose gel electrophoresis (Fig. 3a). The calculated molecular mass was also confirmed when the overexpressed soluble C-His-tagged recombinant Bl-ARC appeared as a band of approximately 56 kDa by SDS/PAGE (Fig. 3b). Western blot was performed (Fig. 3c) to detect the recombinant protein.

Gradient native electrophoresis gel, 5–15%, was performed to detect the migration of the native protein. An apparent oligomeric species of 336 kDa (Fig. 3d) resemble a possible homohexameric complex. We expected Bl-ARC to form a ring conformation such as ReARC, therefore preliminary transmission electron microscopy has been performed on poly-L-lysine grids to confirm the structure (personal communication, Timo Merloo, Department of Cellular and Molecular Medicine, UCSD) at 68 000× magnification. We have so far observed small aggregations and few particle ring patterns, however experiments through particle averaging are needed to confirm the structure.

Nucleotide binding and hydrolysis

Hydrolysis was tested against nucleotides. Bl-ARC has preference to ATP as substrate (100%) when compared against GTP (28%), CTP (31%), and UTP (1.5%). Inhibitors such as ADP, EDTA, *N*-ethylmaleimide (NEM)

Table 1. Effect of inhibitors on Bl-ARC ATPase activity

Inhibitor	mM	% Relative activity
$MgCl_2$ (control)	10	100
EDTA	10	0
NEM	10	3
ADP	1	3
AMPPCP	1	0

Table 2. Divalent metal ion specificity at 1 mM ATP

Metal [10 mM]	% Relative activity*
$MgCl_2$ (control)	100
$MnCl_2$	34
$CuCl_2$	12
$ZnCl_2$	62
$CoSO_4$	9
$CaCl_2$	3

*Nucleotide hydrolyzing activity is expressed as a percentage of the control reaction

H^+-ATPase inhibitor, or α,β-methyleneadenosine 5'-triphosphate sodium salt (AMPPCP) led to a 90% arrest of the ATPase activity (Table 1). Divalent cation metal dependence was measured against Mg^{+2} or Mn^{+2}, Co^{+2}, and Cu^{+2} in Mg^{+2}-free buffer (Table 2). As expected, Bl-ARC showed Mg^{+2}-dependent ATPase actisvity; most of AAA ATPase members require the presence of magnesium ions for their enzymatic catalysis (Briskin and Poole, 1983). This fact in Bl-ARC is related to the presence of the conserved-GKT-sequence in the P-loop, where the lysine residue has a direct contact with Mg^{+2}. Mutation of this residue arrests the activity of most AAA proteins (Liu & Summers, 1988; Carrera *et al.*, 1993; Santos *et al.*, 2004).

Bl-ARC is active in a temperature range of 25–65ºC, however the maximum ATPase activity was observed at 37ºC; this corresponds to the mesophilic nature of *B. longum*. Moreover, the enzyme remained stable at a wide pH range, with preferential activity in the acidic pH (1–6) and a maximum activity was reached at pH 5.0. Interestingly, evidence of pH measurements of feces from bottle-fed infants was found to be >7.0 *versus* breast-fed infants with <6.0 during the first 7 weeks after birth, thus producing an important inhibition of undesirable intestinal bacteria by the presence of bifidobacteria (Lee & O'Sullivan, 2010). Adults possess intraluminal pH of small intestine of 6 to about pH 7.4 in the terminal ileum (Fallingborg, 1999); therefore it has been proposed the use bifidobacterial supplementation in the diet.

Michaelis-Menten plot showed a K_m value of 327 μM and V_{max} of 492 pmol of ATP hydrolyzed per μg of Bl-ARC per min. These parameters are comparable to AAA ReARC and MjPAN (Table 3).

We found that Bl-ARC is an active AAA ATPase. The *bl-arc* gene in *B. longum* genome (Sela *et al.*, 2008) was found in a close proximity to the accessory genes *pup*, *pafA* and *dop* involved in the mechanism of pupylation. This suggests a possible AAA unfoldase activity for target substrates prior to degradation. The functional mechanism of ARC in *B. longum* needs to be further investigated at a molecular and cellular level, along with its role in the maintenance of homeostasis within the host.

Acknowledgements

Mabel Guzmán-Rodríguez was supported by CONACYT graduate scholarship No. 263350. This work was financed by the sectorial grant SEP-101568 from CONACYT, Mexico.

REFERENCES

Bar-Nun S, Glickman MH (2012) Proteasomal AAA-ATPases: structure and function. *Biochim biophys acta* **1823**: 67–82.

Barandun J, Delley CL, Weber-Ban E (2012) The pupylation pathway and its role in mycobacteria. *BMC Biol* **10**: 95.

Benaroudj N, Zwickl P, Seemuller E, Baumeister W, Goldberg AL (2003) ATP hydrolysis by the proteasome regulatory complex PAN serves multiple functions in protein degradation. *Mol Cell* **11**: 69–78.

Briskin DP, Poole RJ (1983) Role of magnesium in the plasma-membrane ATPase of red beet. *Plant Physiol* **71**: 969–971.

Carrera AC, Alexandrov K, Roberts TM (1993) The conserved lysine of the catalytic domain of protein-kinases is actively involved in the phosphotransfer reaction and not required for anchoring ATP. *Proc Natl Acad Sci USA* **90**: 442–446.

Cerda-Maira FA, Pearce MJ, Fuortes M, Bishai WR, Hubbard SR, Darwin KH (2010) Molecular analysis of the prokaryotic ubiquitin-like protein (Pup) conjugation pathway in *Mycobacterium tuberculosis*. *Mol Microb* **77**: 1123—1135.

Delcenserie V, Lessard MH, LaPointe G, Roy D (2008) Genome comparison of *Bifidobacterium longum* strains NCC2705 and CRC-002 using suppression subtractive hybridization. *FEMS Microbiol Lett* **280**: 50–56.

DeMartino GN (2009) PUPylation: something old, something new, something borrowed, something Glu. *Trends Biochem Sci* **34**: 155–158.

Djuranovic S, Hartmann MD, Habeck M, Ursinus A, Zwickl P, Martin J, Lupas AN, Zeth K (2009) Structure and activity of the N-terminal substrate recognition domains in proteasomal ATPases. *Mol Cell* **34**: 580–590.

Table 3. Biochemical features of several AAA ATPase members

AAA protein	K_m (μM)	V_{max} (pmol/min per μg)	Ion dependence	Temp (ºC)	pH	NEM inhibition	Nucleotide dependence	Reference
Bl-ARC	327	492	Mg^{+2}/ Zn^{+2}	37	5.0	+	ATP	This work
ReARC	200	268	Mg^{+2}	30	7.8	+	ATP/CTP	(Wolf *et al.*, 1998)
MjPAN	497	350	Mg^{+2}	80	8–10	+	ATP/CTP	(Wilson *et al.*, 2000)
ScCDC48	550	1560	Mg^{+2}	–	9.0	+	ATP	(Frohlich *et al.*, 1995)
EcFtsH	83	459×10^3	Zn^{+2}	37	–	+	ATP/CTP/GTP	(Tomoyasu *et al.*, 1993)

Doyle SM, Genest O, Wickner S (2013) Protein rescue from aggregates by powerful molecular chaperone machines. *Nat Rev Mol Cell Biol* **14**: 617–629.

Fallingborg J (1999) Intraluminal pH of the human gastrointestinal tract. *Dan Med Bull* **46**: 183–196.

Frickey T, Lupas A (2004) CLANS: a Java application for visualizing protein families based on pairwise similarity. *Bioinformatics* **20**: 3702–3704.

Frohlich KU, Fries HW, Peters JM, Mecke D (1995) The ATPase activity of purified CDC48p from *Saccharomyces cerevisiae* shows complex dependence on ATP-, ADP-, and NADH-concentrations and is completely inhibited by NEM. *Biochim Biophys Acta* **1253**: 25–32.

Guy L, Karamata D, Moreillon P, Roten CA (2005) Genometrics as an essential tool for the assembly of whole genome sequences: the example of the chromosome of *Bifidobacterium longum* NCC2705. *BMC Microbiol* **5**: 60.

Hao Y, Huang D, Guo H, Xiao M, An H, Zhao L, Zuo F, Zhang B, Hu S, Song S, Chen S, Ren F (2011) Complete genome sequence of *Bifidobacterium longum* subsp. longum BBMN68, a new strain from a healthy chinese centenarian. *J Bacteriol* **193**: 787–788.

Hiramatsu Y, Hosono A, Konno T, Nakanishi Y, Muto M, Suyama A, Hachimura S, Sato R, Takahashi K, Kaminogawa S (2011) Orally administered *Bifidobacterium* triggers immune responses following capture by CD11c(+) cells in Peyer's patches and cecal patches. *Cytotechnology* **63**: 307–317.

Kress W, Maglica Z, Weber-Ban E (2009) Clp chaperone-proteases: structure and function. *Res Microbiol* **160**: 618-628.

Lanzetta PA, Alvarez LJ, Reinach PS, Candia OA (1979) An improved assay for nanomole amounts of inorganic phosphate. *Anal Biochem* **100**: 95–97.

Lee JH, O'Sullivan DJ (2010) Genomic insights into *Bifidobacteria*. *Microbiol Mol Biol Rev* **74**: 378–416.

Liu QY, Summers WC (1988) Site-directed mutagenesis of a nucleotide-binding domain in Hsv-1 thymidine kinase-effects on catalytic activity. *Virology* **163**: 638–642.

Marteau P, Pochart P, Flourie B, Pellier P, Santos L, Desjeux JF, Rambaud JC (1990) Effect of chronic ingestion of a fermented dairy product containing *Lactobacillus acidophilus* and *Bifidobacterium bifidum* on metabolic activities of the colonic flora in humans. *Am J Clin Nutr* **52**: 685–688.

Meng EC, Pettersen EF, Couch GS, Huang CC, Ferrin TE (2006) Tools for integrated sequence-structure analysis with UCSF Chimera. *BMC Bioinformatics* **7**: 339.

Ogura T, Wilkinson AJ (2001) AAA+ superfamily ATPases: common structure — diverse function. *Genes Cells* **6**: 575–597.

Olivares M, Laparra M, Sanz Y (2011) Influence of *Bifidobacterium longum* CECT 7347 and gliadin peptides on intestinal epithelial cell proteome. *J Agric Food Chem* **59**: 7666–7671.

Osman N, Adawi D, Molin G, Ahrne S, Berggren A, Jeppsson B (2006) *Bifidobacterium infantis* strains with and without a combination of oligofructose and inulin (OFI) attenuate inflammation in DSS-induced colitis in rats. *BMC Gastroenterol* **6**: 31.

Reddy BS (1999) Possible mechanisms by which pro- and prebiotics influence colon carcinogenesis and tumor growth. *J Nutr* **129**: 1478S–1482S.

Reuter CJ, Kaczowka SJ, Maupin-Furlow JA (2004) Differential regulation of the PanA and PanB proteasome-activating nucleotidase and 20S proteasomal proteins of the haloarchaeon *Haloferax volcanii*. *J Bacteriol* **186**: 7763–7772.

Roy A, Kucukural A, Zhang Y (2010) I-TASSER: a unified platform for automated protein structure and function prediction. *Nat Protoc* **5**: 725–738.

Roy A, Yang J, Zhang Y (2012) COFACTOR: an accurate comparative algorithm for structure-based protein function annotation. *Nucleic Acids Res* **40**: W471–W477.

Ruiz L, Coute Y, Sanchez B, de los Reyes-Gavilan CG, Sanchez JC, Margolles A (2009) The cell-envelope proteome of *Bifidobacterium longum* in an *in vitro* bile environment. *Microbiology* **155**: 957–967.

Samanovic MI, Li H, Darwin KH (2013) The Pup-proteasome system of *Mycobacterium tuberculosis*. *Subcell Biochem* **66**: 267–295.

Santos L, Frickey T, Peters J, Baumeister W, Lupas A, Zwickl P (2004) *Thermoplasma acidophilum* TAA43 is an archaeal member of the eukaryotic meiotic branch of AAA ATPases. *Biol Chem* **385**: 1105–1111.

Schell MA, Karmirantzou M, Snel B, Vilanova D, Berger B, Pessi G, Zwahlen MC, Desiere F, Bork P, Delley M, Pridmore RD, Arigoni F (2002) The genome sequence of *Bifidobacterium longum* reflects its adaptation to the human gastrointestinal tract. *Proc Natl Acad Sci USA* **99**: 14422–14427.

Sela DA, Chapman J, Adeuya A, Kim JH, Chen F, Whitehead TR, Lapidus A, Rokhsar DS, Lebrilla CB, German JB, Price NP, Richardson PM, Mills DA (2008) The genome sequence of *Bifidobacterium longum* subsp. infantis reveals adaptations for milk utilization within the infant microbiome. *Proc Natl Acad Sci USA* **105**: 18964–18969.

Shkoporov AN, Efimov BA, Khokhlova EV, Chaplin AV, Kafarskaya LI, Durkin AS, McCorrison J, Torralba M, Gillis M, Sutton G, Weibel DB, Nelson KE, Smeianov VV (2013) Draft genome sequences of two pairs of human intestinal *Bifidobacterium longum* subsp. longum Strains, 44B and 1-6B and 35B and 2-2B, consecutively isolated from two children after a 5-year time period. *Genome Announc* **1**.

Smith DM, Kafri G, Cheng Y, Ng D, Walz T, Goldberg AL (2005) ATP binding to PAN or the 26S ATPases causes association with the 20S proteasome, gate opening, and translocation of unfolded proteins. *Mol Cell* **20**: 687–698.

Striebel F, Imkamp F, Sutter M, Steiner M, Mamedov A, Weber-Ban E (2009a) Bacterial ubiquitin-like modifier Pup is deamidated and conjugated to substrates by distinct but homologous enzymes. *Nat Struct Mol Biol* **16**: 647–651.

Striebel F, Kress W, Weber-Ban E (2009b) Controlled destruction: AAA+ ATPases in protein degradation from bacteria to eukaryotes. *Curr Opin Struct Biol* **19**: 209–217.

Sugimoto S, Sonomoto K (2011) Quality control of protein structure in lactic acid bacteria. In *Lactic Acid Bacteria and Bifidobacteria*: *Current Progress in Advanced Research*, pp 143–154. Caister Academic Press, Hokkaido, Japan.

Sun Z, Bo X, He X, Jiang Z, Wang F, Zhao H, Liu D, Yuan J (2008) Comparative proteome analysis of *Bifidobacterium longum* NCC2705 grown on fructose and glucose. *Sheng Wu Gong Cheng Xue Bao* **24**: 1401–1406.

Sutter M, Striebel F, Damberger FF, Allain FH, Weber-Ban E (2009) A distinct structural region of the prokaryotic ubiquitin-like protein (Pup) is recognized by the N-terminal domain of the proteasomal ATPase Mpa. *FEBS Lett* **583**: 3151–3157.

Tanaka K (2009) The proteasome: overview of structure and functions. *Proc Jpn Acad Ser B Phys Biol Sci* **85**: 12–36.

Tissier H (1900) Recherches sur la flore intestinale normale et pathologique du nourisson. These de Paris:1–253.

Tomoyasu T, Yuki T, Morimura S, Mori H, Yamanaka K, Niki H, Hiraga S, Ogura T (1993) The *Escherichia coli* FtsH protein is a prokaryotic member of a protein family of putative ATPases involved in membrane functions, cell cycle control, and gene expression. *J Bacteriol* **175**: 1344–1351.

Vale RD (2000) AAA proteins: Lords of the ring. *J Cell Biol* **150**: F13–F19.

Wang T, Li H, Lin G, Tang C, Li D, Nathan C, Darwin KH (2009) Structural insights on the *Mycobacterium tuberculosis* proteasomal ATPase Mpa. *Structure* **17**: 1377–1385.

Wilson HL, Ou MS, Aldrich HC, Maupin-Furlow J (2000) Biochemical and physical properties of the *Methanococcus jannaschii* 20S proteasome and PAN, a homolog of the ATPase (Rpt) subunits of the eucaryal 26S proteasome. *J Bacteriol* **182**: 1680–1692.

Wolf S, Nagy I, Lupas A, Pfeifer G, Cejka Z, Muller SA, Engel A, De Mot R, Baumeister W (1998) Characterization of ARC, a divergent member of the AAA ATPase family from *Rhodococcus erythropolis*. *J Mol Biol* **277**: 13–25.

Xu JR, Zhang Y (2010) How significant is a protein structure similarity with TM-score=0.5? *Bioinformatics* **26**: 889–895.

Yu H, Liu L, Chang Z, Wang S, Wen B, Yin P, Liu D, Chen B, Zhang J (2013) Genome sequence of the bacterium *Bifidobacterium longum* strain CMCC P0001, a probiotic strain used for treating gastrointestinal disease. *Genome Announc* **1**.

Yuan J, Zhu L, Liu X, Li T, Zhang Y, Ying T, Wang B, Wang J, Dong H, Feng E, Li Q, Wang J, Wang H, Wei K, Zhang X, Huang C, Huang P, Huang L, Zeng M, Wang H (2006) A proteome reference map and proteomic analysis of *Bifidobacterium longum* NCC2705. *Mol Cell Proteomics* **5**: 1105–1118.

Zhang X, Stoffels K, Wurzbacher S, Schoofs G, Pfeifer G, Banerjee T, Parret AH, Baumeister W, De Mot R, Zwickl P (2004) The N-terminal coiled coil of the *Rhodococcus erythropolis* ARC AAA ATPase is neither necessary for oligomerization nor nucleotide hydrolysis. *J Struct Biol* **146**: 155–165.

Zhang Y (2008) I-TASSER server for protein 3D structure prediction. *BMC bioinformatics* **9**: 40.

Zhao J, Cheung PC (2013) Comparative proteome analysis of *Bifidobacterium longum* subsp. infantis grown on beta-glucans from different sources and a model for their utilization. *J Agric Food Chem* **61**: 4360–4370.

Zhurina D, Dudnik A, Waidmann MS, Grimm V, Westermann C, Breitinger KJ, Yuan J, van Sinderen D, Riedel CU (2013) High-quality draft genome sequence of *Bifidobacterium longum* E18, isolated from a healthy adult. *Genome Announc* 1.